International Journal of Advanced Research and Development
ISSN: 2455-4030
Impact Factor: RJIF 5.24
www.advancedjournal.com
Volume 2; Issue 6; November 2017; Page No. 513-524

Spectroscopic (FT-IR and FT-Raman, UV, NMR, NBO and NLO) Analysis and DFT Computations of 2Chloro-5-Trifluoromethyl Pyridine

[1] R Sangeetha, [*2] S Seshadri, [3] Rasheed MP

[1] Research Scholar, PG and Research Department of Physics, Urumu Dhanalakshmi College, Trichy, Tamil Nadu, India
[2] Associate Professor and Head, PG and Research Department of Physics, Urumu Dhanalakshmi College, Trichy, Tamil Nadu, India
[3] Research Scholar, PG and Research Department of Physics, Urumu Dhanalakshmi College, Trichy, Tamil Nadu, India

Abstract
In this work, the vibrational spectral analysis was carried out using Raman and Infrared spectroscopy (solid phase) in the range 4000-400cm^{-1} and 3500 cm^{-1}, respectively, for the 2-Chloro-5-Trifluoromethyl pyridine (2C5TFMP).Simulation of Infrared and Raman spectra utilizing the results of these calculations led to good agreement with the observed spectral patterns. The complete assignments were performed on the basis of the potential energy distribution (PED) of the vibrational modes, calculated with scaled quantum mechanics (SQM) method. The molecular structure and fundamental vibrational frequencies have been obtained from density functional theory (DFT) B3LYP methods with 6-311++G (d, p) basis set calculations. The investigation in view of NMR chemical shift, First Order Hyperpolarizability, Molecular Electrostatic Potential Map (MESP) and Thermo dynamical functions have been carried out. The observed HOMO LUMO mappings reveal the charge transfer possibilities within the molecule. Natural Bond Orbital analysis, Mulliken charges, electrostatic potential charges are also computed.

Keywords: HOMO LUMO, DFT, hyperpolarizability, Mulliken charges

1. Introduction
Pyridine is a heterocyclic fragrant compound filling in as the parent compound of numerous biologically significant derivatives. It has been used very frequently as a proton acceptor in studies involving hydrogen bonded complexes [1, 2]. Vibrational spectra of substituted pyridine got extensive consideration in the spectroscopic perspective of their obvious significance to natural frameworks and mechanical criticalness [3, 8]. Pyridine heterocycles and its derivatives are a repeated moiety in many large molecules with interesting photo chemical, electrochemical and catalytic applications [9, 11]. To the best of our knowledge, neither the vibrational analysis nor the quantum chemical study of 2Chloro-5-Trifluoromethyl pyridine has been reported.

2. Materials and Methods
The compound under investigation 2C5TFMP namely was procured from Sigma–Aldrich chemicals, U.S.A with a stated purity of greater than 98%. The compound was used as such without further purification. The FT-IR spectrum of the compound was recorded in the region 3500-400cm-1 on a Perkin Elmer FT-IR Spectrophotometer. The FT-Raman spectrum of the title compound was recorded in the Bruker FRA 106/S instrument equipped with Nd: YAG laser source operating at 1064 nm line widths in the range of 3500–100cm^{-1}.

2.1 Quantum chemical calculations
The gas phase geometry of the compound under investigation (2C5TFMP) in the ground state was optimized by using DFT/B3LYP(Becke3–Lee–Yang–Parr) level with the standard basis set 6-311++G(d,p) using Gaussian 09W [12] program package, invoking gradient geometry optimization [13]. The scaling factors have to be used to obtain considerably better agreement with experimental data.

2.2 Prediction of Raman Intensities
The Raman activities (Si) calculated with the GAUSSIAN 09 program and adjusted during the scaling procedure with MOLVIB were subsequently converted to relative Raman intensities (Ii) using the following relationship(1) derived from the basic theory of Raman scattering [14, 15].

$$I_i = \frac{f(\nu_o - \nu_i)^4 S_i}{\nu_i\left[1 - \exp\left(\frac{-hc\nu_i}{kT}\right)\right]} \qquad (1)$$

Where ν_0 is the exciting frequency (in cm-1 units); ν_i is the vibrational wave number of the of the ith normal mode, h, c and k are fundamental constants and f is a suitably chosen common normalization factor for all peaks intensities. Raman activities and calculated Raman intensities are reported in Table.2.

3. Results and Discussion
3.1 Molecular Geometry
Initial geometry generated from standard geometrical parameters was optimized and equilibrium geometry has been determined by the energy minimization. The ground state optimized structure of the molecule is presented in Fig.1.The optimized structure of 2C5TFMP and experimental structures

of 2C5TFMP were compared. The agreement between the optimized and experimental structure is quite good displaying that the geometry optimization almost exactly reproduces the experimental conformation.

The geometry of a molecule can be characterised by analysing the bond length and bond length. Using B3LYP 6-311++G (d, p) basis set, bond length and bond angle values are collected in Table.1.

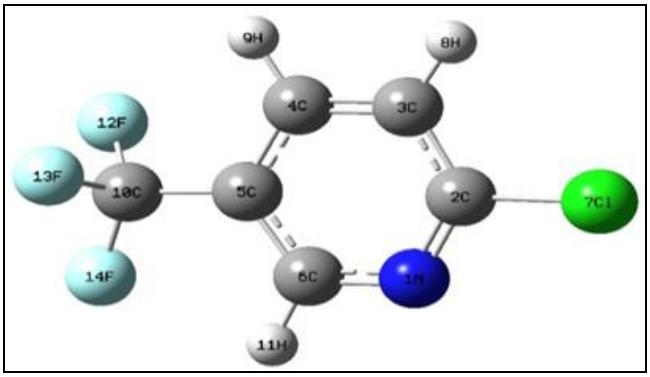

Fig 1: Molecular structure of 2C5TFMP along with numbering of atoms

Table 1: Optimized geometrical parameters of 2C5TFMP obtained by B3LYP/6-311++G (d,p) density functional calculations.

Bond length	Angstrom (Å)	Bond angle	Degree	Torsional angle	Degree
N1-C2	1.347969	F14-C10-C5	112.3353	14F-C10-C5-C4	166.8419
C3-C2	1.355865	F13-C10-C5	111.6221	13F-C10-C5-C4	-72.9217
C4-C3	1.35355	F12-C10-C5	111.6616	F12-C10-C5-C4	46.10811
C5-C4	1.083666	H11-C6-N1	116.2919	H11-C6-N1-C2	179.7867
C6-N1	1.502704	C10-C5-C4	120.1091	C10-C5-C4-C3	178.4774
Cl7-C2	1.083468	H9-C4-C3	120.4245	H9-C4-C3-C2	-179.739
H8-C3	1.081202	H8-C3-C2	120.8779	H8-C3-C2-N1	-179.765
H9-C4	1.754942	Cl7-C2-N1	116.7387	CL7-C2-N1-C6	179.9631
C10-C5	1.3376	C6-N1-C2	117.7072	C6-N1-C2-C3	-0.12884
H11-C6	1.397759	C5-C4-C3	118.9415	C5-C4-C3-C2	-0.13653
F12-C10	1.38475	C4-C3-C2	117.3186	C4-C3-C2-N1	0.149576
F13-C10	1.398179	C3-C2-N1	124.6615	14F-C10-C5-C4	166.8419
F14-C10	1.316136	F14-C10-C5	112.3353	13F-C10-C5-C4	-72.9217
N1-C2	1.347969	F13-C10-C5	111.6221	F12-C10-C5-C4	46.10811
C3-C2	1.355865	F14-C10-C5	112.3353		
C4-C3	1.35355				
C5-C4	1.083666				

The comparative IR and Raman spectra of experimental and calculated frequencies are given in the Fig.2 and Fig.3

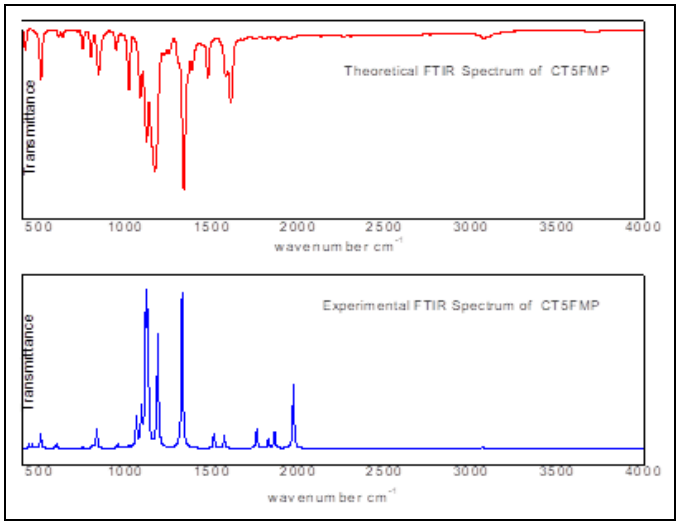

Fig 2: Comparison of Theoretical and Experimental FTIR spectrum of 2C5TFMP

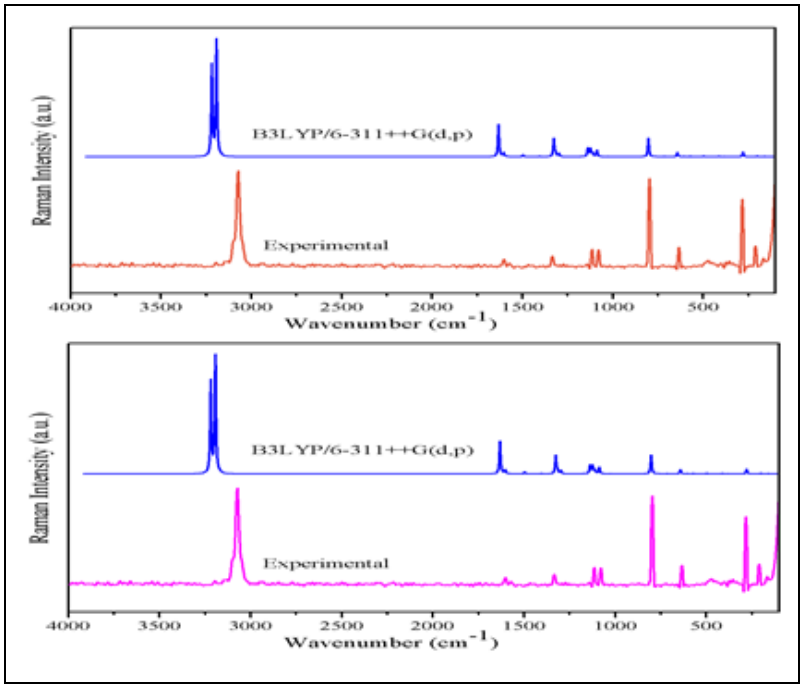

Fig 3: Comparison of Theoretical and experimental FT-Raman spectrum of 2C5TFMP

3.2 Vibrational Assignment

The present work involves satisfactory vibrational band assignments for the title molecule in terms of normal modes of vibration using FTIR and FT Raman spectroscopy. The title compound has (3N-6) 36 normal vibrational modes. All the vibrational frequency calculations were carried out after optimizing the structure of the molecule to its minimum energy. It is well known that the DFT method predicts vibrational calculations with high accuracy which is applicable to larger number of compounds.

The experimental FTIR and FT-Raman spectrum are presented in Fig.2 and Fig.3.The experimental and calculated wavenumbers and their assignments along with PED (Potential Energy Distribution) of the title compound are given in Table.2. Electron correlation effects, insufficient basis sets to describe the molecular orbital exactly and anharmonicity are some of the important factors which results in higher values of calculated wavenumbers than the corresponding experimental ones. These discrepancies are removed either by computing anharmonic corrections explicitly or by introducing scalar field or even by direct scaling of the calculated wavenumbers with a proper scaling factor [16, 17].

To assign bands in the experimental vibrational spectra to molecular fragments one has to recognize which atoms play a dominant role in the normal modes corresponding to the bands in calculated spectra. With an increase in the number of normal modes, the number of fragments that may contribute to a mode increase quickly. PED (potential energy distribution) evaluation is using MOLVIB program is used to indicate in which mode a given fragment is participating. Most of the fragments participate in several different modes. Such an analysis determines a potential energy connected with molecular fragments. The complete detail of the PED analyses can be found elsewhere [18, 19]. The various vibrational modes of the title molecule are discussed as under.

3.2.1 C-H Stretching Vibrations

The C-H stretching vibrations are normally observed in the region 3100-3000cm^{-1} for aromatic benzene structure [20, 21] which shows their uniqueness of the skeletal vibrations. The bands appeared at 3073.62cm^{-1} in FTIR and 3072.63cm^{-1} in FT Raman in the present sample have been assigned to C-H stretching vibrations. It's theoretically computed values for C-H stretching vibrations of 2C5TFMP are found to be 3191.70, 3193.41, 3217.97cm^{-1} respectively. These stretching vibrations are scaled to 3060.1, 3061.7, 3086.0cm^{-1} with a maximum 99% PED contribution.

The CH in-plane bending normally occurred as a number of strong to weak intensity bands in the region 1300-1000cm^{-1}. When there is in-plane interaction above 1200cm^{-1}, a carbon and its hydrogen usually move in opposite direction [22]. Accordingly for our title compound, the C-H in-plane bending vibrations occur at 1604.78, 1574.81, 1471.69 and 1379.91cm^{-1} in FTIR and 1334.59, 1602.97cm^{-1} in FTRaman spectrum respectively.

According to literature survey, the C-H out-of-plane bending vibrations normally appear in the region1000-809 cm^{-1} [23]. In this work, the C-H out-of-plane bending vibrations occur at 794, 838, 940, 1015 cm^{-1} in IR spectrum. Here we have theoretically calculated values such as 751, 847, 962 and 992 cm^{-1} which shows that the predicted values are found to be nearly equal to the observed frequencies.

3.2.2 C-C Vibrations

The experimental and theoretical skeletal (ring CC) vibrations were assigned in the region 915-1630cm^{-1} [24]. In this present work, the C-C stretching vibrations are appeared at 1471, 1379 and 1248 in FTIR and 1334 cm^{-1} in FT Raman respectively. Socrates [25] mentioned that, the presence of

conjugate substituent such as C=C causes stretching peaks around the region 1625-1575cm^{-1}. As predicted in the earlier references, in this title compound, the prominent peaks are found with strong and medium intensity 1574cm^{-1} in FTIR due to C=C stretching vibrations.

Table 2: Observed and B3LYP/6-311++G (d,p) level calculated vibrational frequencies (in cm^{-1}) of 2C5TFMP

No	Symmetry Species	Observed frequency		Calculated frequency (cm^{-1})with B3LYP/6-311++G(d,p) force field				Characterisation of normal modes with PED%
		IR (cm^{-1})	Raman (cm^{-1})	Unscaled (cm^{-1})	Scaled (cm^{-1})	IR intensity	Raman activity Si	
1	A"	--	--	19.4654	61.9	1.4418	2.6414	tCF (63)
2	A"	--	72.64	75.4697	80.3	0.8472	1.6745	tCCl (58)
3	A'	--	--	158.8064	155.3	2.2262	0.6219	tCF (99)
4	A"	--	210.34	201.7518	199.3	0.1173	1.1540	bCC (35),bCCF (32),bCCl(13)0
5	A'	--	282.54	278.4882	278.3	0.1617	6.0199	CC(39),bring(34),CCl(15)
6	A'	--	--	309.2505	293.4	0.6378	0.1232	bCC (47),bCCl(25)
7	A"	--	354.08	383.2601	354.6	0.4759	0.4024	tCF3(39), tring(35),bCCF(22)
8	A'	414.46	--	411.8119	417.9	4.1831	1.0174	tring(69), tCF3(16), gCH(13)
9	A'	--	--	425.5648	454.0	7.1557	0.0631	tCF3(38), bCCF(26),bCC(13)
10	A"	--	475.83	496.3698	495.7	39.7929	0.9586	tCF3(68), tring(23)
11	A'	505.61	--	500.4337	503.7	3.2809	0.3026	CCl(56), CC(21), bring(12),
12	A'	--	--	571.0736	574.2	0.6385	0.7958	CF(33), tCF3 (21), bCCF (17), CC(11)
13	A"	--	--	604.8991	609.5	2.6156	0.6415	tCF3(35), tring(28), bCCF(19), CF(11)0
14	A'	632.13	633.90	641.7977	634.5	1.0101	5.5387	bring(78),CC(10)
15	A"	746.7	--	714.0417	718.4	0.0564	0.6648	CF(40), bCCF(29), bring(17)
16	A"	794.76	--	759.4145	761.7	4.8352	0.1753	tring(46),tCF3(33),gCH(14)
17	A'	--	--	802.0443	794.4	9.9640	23.5553	bring (41),CC(28), CCl (14), CF(13)
18	A"	838.67	--	847.8130	844.4	32.7032	0.1358	gCH(67),tCF3(23)
19	A'	940.09	--	962.3323	928.4	12.6452	0.1228	gCH(90)
20	A"	1015.15	--	992.3282	953.6	0.3280	0.0270	gCH(84)
21	A'	--	--	1025.7407	1010.5	73.77	0.2839	bring (69), CC (19)
22	A'	1080.56	1078.40	1086.8498	1086.1	1086.84	8.5923	CC(53), CF(23), bCCF(16)
23	A"	--	1114.43	1110.8772	1111.0	1110.87	4.4180	CF (49), tCF3 (28), bCCF (21)
24	A'	--	--	1122.7089	1115.3	1122.70	10.1340	CF(51), CC(21), tCF (12), bCCF (10)
25	A'	--	--	1137.5374	1128.6	1137.53	11.0763	CC (41), CCl(18),CF(12), bring(10)
26	A'	--	--	1172.1378	1176.3	1172.13	0.3491	CC(79)
27	A'	1248.56	--	1297.2216	1250.2	1297.22	4.2819	CC(61), bCCF (14),CF(12)0
28	A'	--	--	1316.0355	1306.1	1316.03	3.9530	CC(33),bCC(17),CN(13),bCH(12), bCCF(12)
29	A'	1379.91	1334.59	1325.5002	1330.1	1325.50	22.9889	bCH(31),CN(27),CC(18), bNCH(10)
30	A'	1471.69	--	1405.2677	1405.5	1405.26	0.7311	bCH (63),CC(18)
31	A'	1574.81	--	1496.4247	1500.3	1496.42	2.6447	bCH (67),CC(15)
32	A'	1604.78	1602.97	1602.8481	1590.4	1602.84	4.8296	bCH(42),CN(38)
33	A'	1877.75	--	1831.4094	1625.0	1631.40	40.9588	CN(76), bCH (10)
34	A'	--	3072.63	3191.7061	3060.1	3191.70	87.3353	CH(99)
35	A'	--	--	3193.4173	3061.7	3193.41	65.3814	CH (99)
36	A'	3073.62	--	3217.9745	3086.0	3217.97	114.4591	CH (99)

(υ) stretching (b)bending; (g) scissoring and wagging ; (t) torsion ;PED values are greater than 10% are given

3.2.4 C-Cl Vibrations

In the present investigation, due to the presence of heavy atoms (Chlorine and Fluorine) on the periphery of the molecule mixing of vibrations are possible. Mooney [29] assigned of C-X group (X=Cl, Br, I) in the frequency range of 1129-480cm^{-1}. The C-Cl stretching vibrations of the title compound is assigned by the presence of a band at 505cm^{-1} in FTIR and 282cm^{-1} in FT Raman and 500 and 278cm^{-1} by B3LYP is well correlated with the experimental observations.

3.2.5 CF3 Vibration

The title molecule 2C5TFMP under consideration possesses one CF3 group in the fifth position of the ring. The bands are appeared at 746.7 cm^{-1} in FTIR and 1114.43 cm^{-1} in FT-Raman is assigned to C-F stretching vibration.

The in-plane bending mode for CF stretching is observed at 210.34, 1078.40 and 1114.43cm^{-1} in FT Raman and 1248.56, 1080.56 cm^{-1} in FTIR spectrum. The scaled experimental values for in-plane bending vibrations assigned at 199.3, 1086.1, 1111 and 1250.2.The experimental values coincide well with the observed values.

CF3 rocking mode usually appears in the ranges of 450-350cm^{-1} and 350-260cm^{-1} [30]. Hence, in our title compound, the band appears at 354.08 cm^{-1} in FT Raman ensures the presence of CF3 rocking mode. It is difficult to observe the torsional motion in the FT-IR and FT-Raman spectra. This is because of the low wave number and also due to the presence of heavier fluoro methyl group.

The experimental values at 475,324 cm^{-1} in FT Raman spectra by B3LYP methods is assigned to CF3 out of plane rocking mode. The theoretically calculated values observed at 496, 383 cm^{-1}. Both the experimental and theoretical values found to be agree with each other.

3.2.6 Ring Vibrations

The ring in-plane and out–of-plane bending vibrations of 2C5TFMP are assigned unambiguously with the help of PED output and Gauss view program. The small changes in

frequencies observed for these modes are due to the changes in force constant reduced mass ratio resulting mainly due to the extent of mixing between ring and substituent group.

3.3 Thermodynamic Properties

Theoretically computed thermodynamic parameters such as energies (a.u), zero point vibrational energies(kcalmol^{-1}), rotational constants (GHz),entropies (cal mol^{-1}) and dipole moment of 2C5TFMP by DFT/B3LYP /6-311++G(d,p) method are listed in Table.4. It can be observed that these thermodynamic functions are increasing with temperature ranging from 100 to 1000 K due to the fact that the molecular vibrational intensities increase with temperature [31, 33]. While performing the calculation, the molecule was considered to be at room temperature of 298.15 K and one atmospheric pressure.

The correlation equation among heat capacity, entropy, enthalpy changes with temperatures were fitted by quadratic formulas and the corresponding fitting factors (R^2) these thermodynamic properties are 0.99956, 0.99984 and 0.99938 respectively. The correlations plot is shown in Fig. 10. The corresponding fitting equations (2), (3) and (4) are given below:

$$\left(C^{\,0}_{p,m}\right) = 25.9038 + 0.6436T - 2.8331 \times 10^{-4}T^2 \quad (R^2 = 0.99956) \quad (2)$$

$$\left(S^{\,0}_{m}\right) = 258.885 + 0.7796T - 2.1163 \times 10^{-4}T^2 \quad (R^2 = 0.99984) \quad (3)$$

$$\left(H^{\,0}_{m}\right) = -8.2479 + 0.09863T - 1.6577 \times 10^{-4}T^2 \quad (R^2 = 0.99938) \quad (4)$$

The thermodynamic functions grant very useful information for the further study on the 2C5TFMP. They can be used to calculate the other thermodynamic energy according to the relationship of thermodynamic functions and evaluate directions of chemical behavior according to the second law of thermodynamics in the thermochemical field [34]. Here, all thermodynamic computation were done in the gas phase and without be used in the solution.

Table 3: The Temperature dependence of Thermodynamic parameters of 2, 3-DC5TFMP

Temperature [T]	Energy[E] (KCal/Mol)	Heat capacity [Cv] (Cal/Mol-kelvin)	Entropy[s] (Cal/Mol-kelvin)
100	47.627	15.094	72.621
200	49.676	25.928	87.769
300	52.790	36.142	101.063
400	56.843	44.579	113.238
500	62.638	51.007	124.354
600	66.991	55.812	134.461
700	72.762	59.452	143.657
800	78.854	62.271	152.053
900	85.197	64.500	159.755
1000	91.739	66.294	166.856

The graph showing the correlation of heat capacity at constant pressure (Cp), entropy (S) and enthalpy change (ΔH0→T) with temperature is delineated in Fig.4, Fig.5 and Fig.6

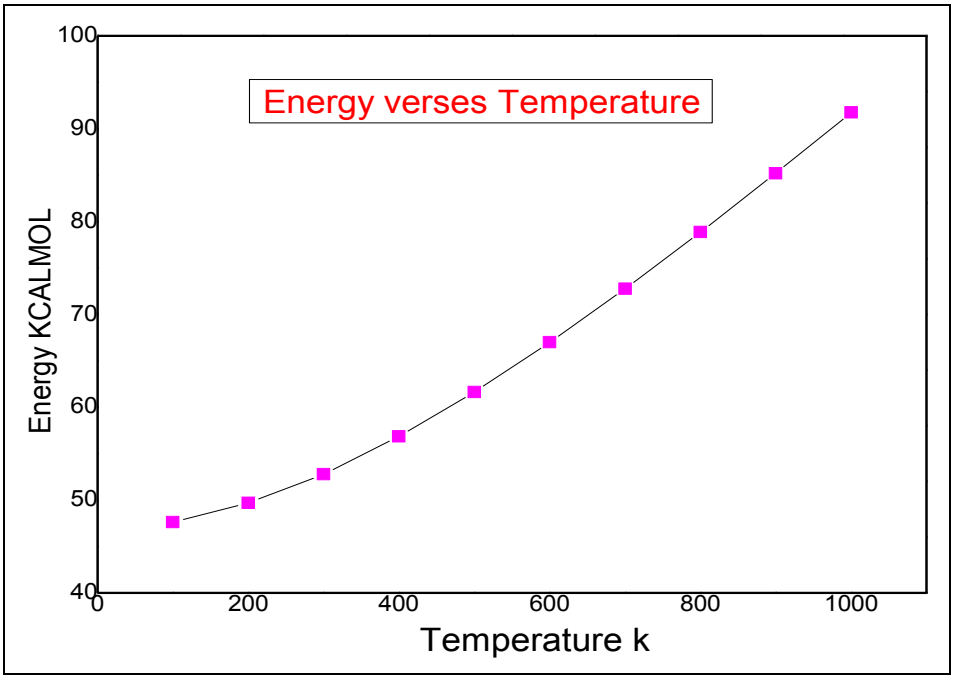

Fig 4: Temperature dependence of energy of 2C5TFMP

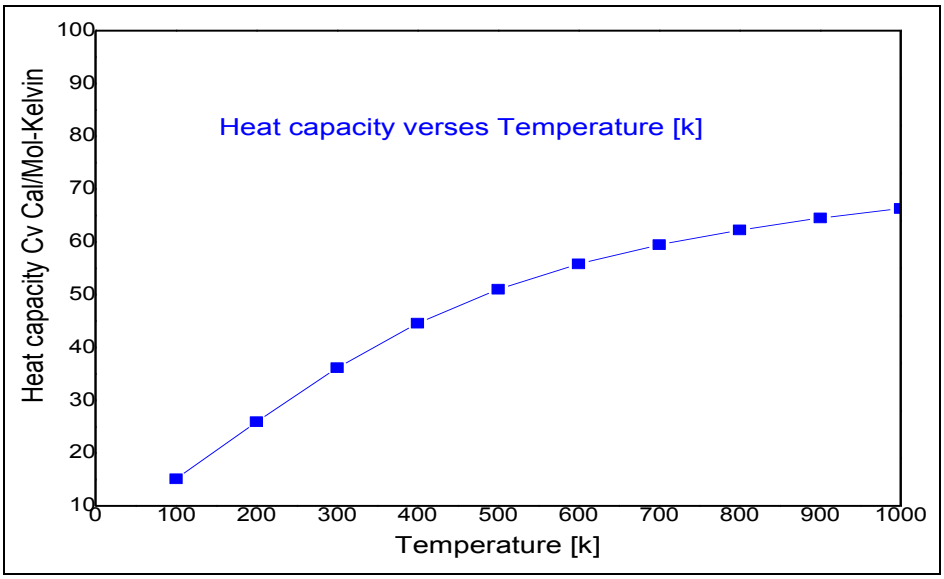

Fig 5: Temperature dependence of Heat capacity at Constant Volume of 2C5TFMP

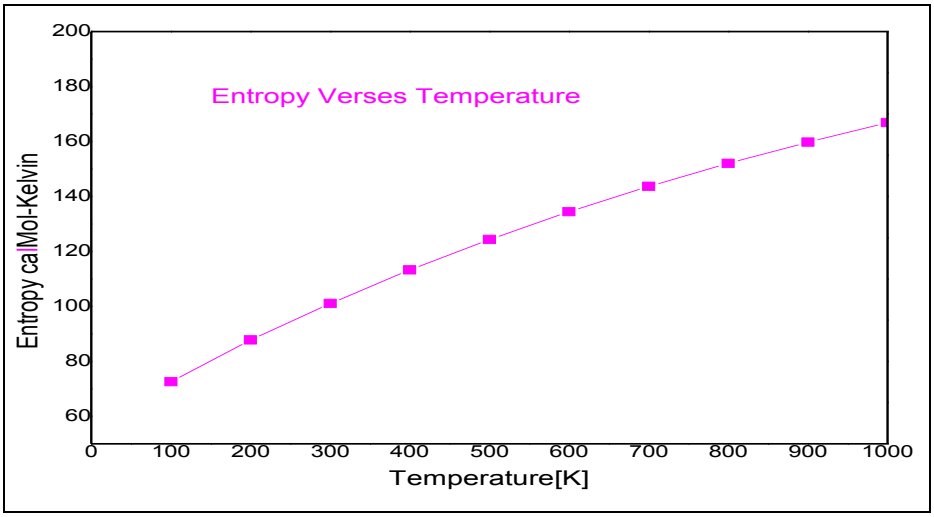

Fig 6: Temperature dependence of Entropy of 2CT5FMP

3.4 HOMO-LUMO Analysis

HOMO and LUMO energy values are very important parameters for quantum chemistry. The HOMO is the orbital primarily acts as an electron donor and the LUMO is the orbital that largely acts as the electron acceptor, and the gap between the HOMO and LUMO characterizes the molecular orbitals is a critical parameter in determining molecular electrical transport properties because it is a measure of electron conductivity. The energy pap between HOMO and LUMO determines the kinetic stability, chemical reactivity and optical polarizability and chemical hardness-softness of a molecule [35].

Molecular orbital and their frontier electron density used for predicting the most reactive position in л-electron system and also explained several types of reaction in conjugated systems [36]. The total energy, energy gap and dipole moment affect on the stability of a molecule. Surfaces for the frontier orbital were drawn to understand the bonding scheme of present compound and it is shown in Fig.7. The computed energies and the energy gap is

HOMO energy = -2.077046162 eV
LUMO energy = 5.894261354 eV
HOMO-LUMO energy gap = -7.971307516 eV

The energy gap between HOMO and LUMO implies that our present compound have high band between the frontier molecular orbitals. A high HOMO-LUMO energy gap shows high kinetic stability and low chemical reactivity since it is energetically unfavourable to add electron to a high lying LUMO by extracting electrons from low lying HOMO.

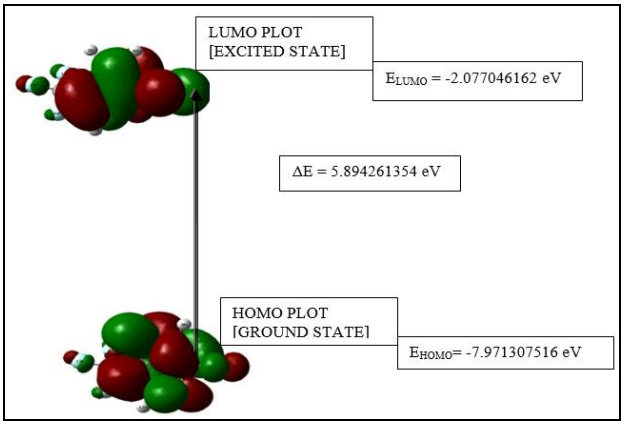

Fig 7: The atomic orbital compositions of the frontier molecular orbital (HOMO-LUMO) for 2C5TFMP

Table 4: Energy values of 2C5TFMP by B3LYP/6 311++G (d, p) method

Energies	Values
E_{HOMO} (eV)	-7.971307516
E_{LUMO} (eV)	-2.077046162
E_{HOMO} - E_{LUMO} gap (eV)	5.894261354
Chemical hardness (η)	2.918025
Softness (S)	0.016956
Electronegativity (χ)	-5.02418
Chemical potential (μ)	5.02418
Electrophilicity index (ω)	4.2853

3.5 Mulliken Charges

The calculation of atomic charges play an important role in the application of quantum mechanical calculations to molecular systems, because the atomic charges affect the dipole moment, polarizability, electronic structure, and much more properties of the molecular systems [37]. Mulliken charges are calculated by determining the electron population of each atom has defined in the basis functions. The charge distributions calculated by the Mulliken for the title compound is collected in Table.5. The charge distribution on the molecule has an important influence in the vibrational spectra.

Table 5: Atomic Charges for optimized geometry of 2C5TFMP using DFT-B3LYP/6-311++G (d, p)

Atoms	Mullikken Atomic Charges
N1	0.110153
C2	-1.02495
C3	0.342092
C4	0.049355
C5	-0.41411
C6	-0.42224
Cl7	0.529923
H8	0.213932
H9	0.226311
C10	0.452526
H11	0.227829
F12	-0.0895
F13	-0.06677
F14	-0.13454

From Table.5, it can be noticed that N1, C3, C4, C10, Cl7, H8,H9 and H11 atoms of 2C5TFMP exhibit positive charge, while C2,C5,C6,F12,F13 and F14 atoms exhibit negative charges. The carbon atoms C2, C5 and C6 exhibit negative charges due to the presence of electron withdrawing property of chlorine and trifluoromethyl group. In addition, the Mulliken atomic charges and histogram of Mulliken charges was shown in Fig.8. and Fig.9.

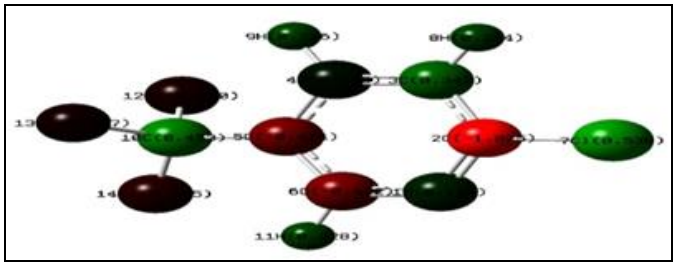

Fig 8: Mulliken atomic charges

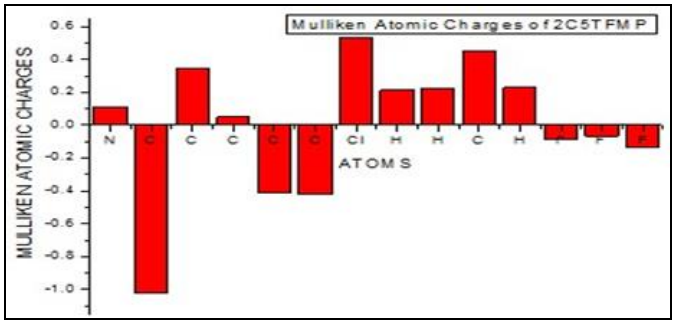

Fig 9: Histogram of calculated Mulliken charges of 2C5TFMP

3.6 Analysis of molecular electrostatic potential (MESP)

The molecular electrical potential surfaces illustrate the charge distributions of molecules three dimensionally. This map allows us to visualize variably charged regions of a molecule. The knowledge of the charge distributions can be used to determine how molecules interact with one another and it is also used to determine the nature of the chemical bonds. Molecular electrostatic potential is calculated at the B3LYP/6-311++G (d, p) for the optimized geometry of the compound [38, 39].

The negative and positive potential regions of the MESP are expected to be the sites of nucleophilic and electrophilic region shown in Fig.10a and Fig.10b is used to visualize

variably charged regions of molecule in terms of colour grading. The red region refers to greatest electron density while the blue region is characterized by electron poor region. The green region in MESP refers to the neutral region of electron density. The electrostatic potential increases in the order red< orange< yellow< green< blue [40]. The colour code of the maps in the range -4.088a.u (deepest red) to 4.088 (deepest blue) in the title molecule, where the blue indicates the strongest attraction and the red colour indicates the strongest repulsion.

The molecular electrostatic potential (MESP) mainly explores the molecular interactions within the molecule. It also provides the correlations between the molecular properties like chemical reactivity and electronegativity of molecules [41]. According to these calculated results, we can conclude that H atoms indicate the strongest attraction. Additionally, the nitrogen atom and chlorine atom has slightly falls in the positive region and the fluorine atoms slightly falls in the negative region.

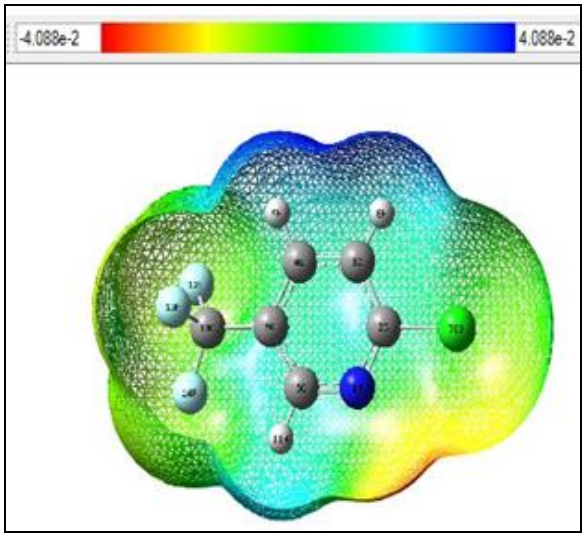

Fig 10(a): Mesh view

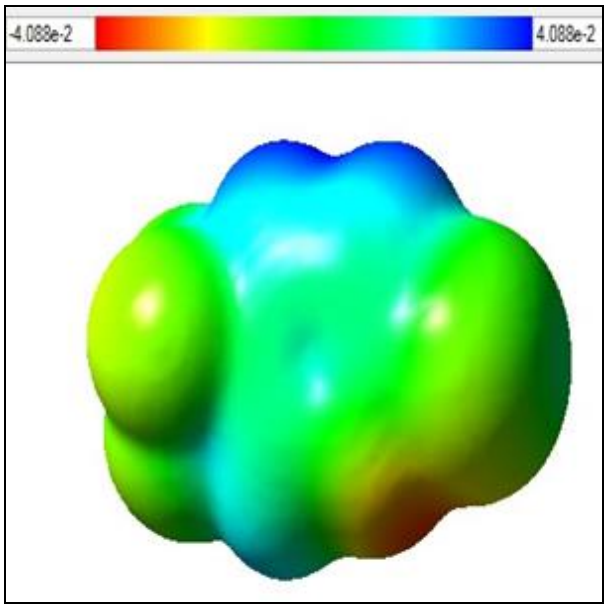

Fig 10(b): Solid view

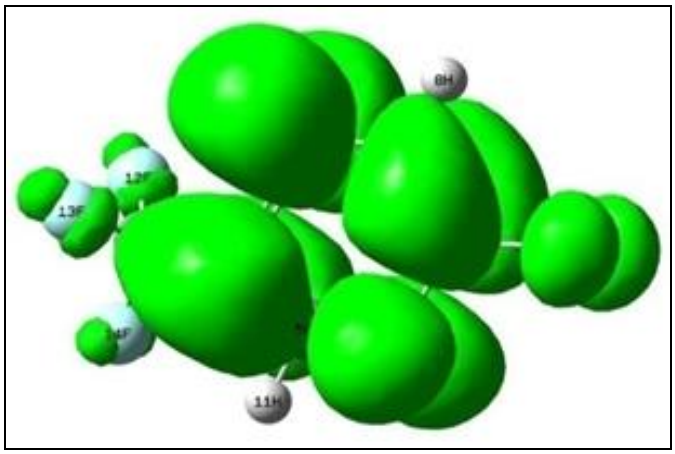

Fig 11: Electron density from total SCF density mapped with esp

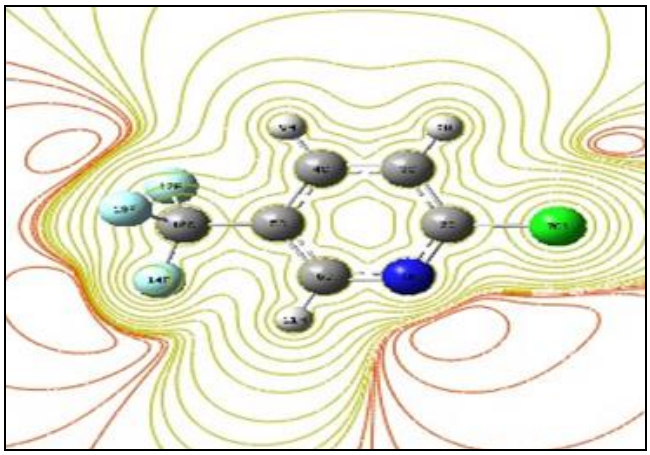

Fig 12: Contour Map of 2C5TFMP

3.7 Natural Bond Orbital Analysis

NBO algorithm calculates all possible donor acceptor combinations and several interactions have been seen in Table.6.

Table 6: Second order perturbation theory analysis of Fock matrix in NBO basis for 2C5TFMP

Donor(i)	Type	ED/e	Acceptor(i)	Type	ED/e	[a]E(2) (KJ mol^{-1})	[b]E(J)-E(i) (a.u.)	[c]F(I,j) (a.u.)
N1-C2	σ	1.9841	N1-C6	σ*	0.0146	1.28	1.41	0.038
N1-C2	σ		C2-C3	σ*	0.05369	2.92	1.39	0.057
N1-C2	π	1.73218	C3-C4	π*	0.33895	11.62	0.33	0.056
N1-C6	σ	1.97687	C2-Cl7	σ*	0.05768	4.7	0.99	0.061
C2-C3	σ	1.98375	C3-C4	σ*	0.02672	3.21	1.31	0.058
C2-Cl7	σ	1.98687	N1-C6	σ*	0.0146	3.27	1.25	0.057
C2-Cl7	σ		C3-C4	σ*	0.05369	2.51	1.26	0.05
C3-C4	σ	1.97419	C2-C3	σ*	0.05369	3.9	1.26	0.063
C3-C4	σ		C2-Cl7	σ*	0.05768	4.32	0.89	0.056
C3-C4	σ		C4-C5	σ*	0.02232	3.16	1.3	0.057
C3-C4	σ	0.42741	N1-C2	σ*	0.03027	25.9	0.27	0.077
C3-C4	σ	0.32997	C5-C6	σ*	0.03	16.05	0.3	0.062
C3-Cl8	σ	1.98848	N1-C2	σ*	0.03027	2.7	1.27	0.052
C4-C5	σ	1.96715	C3-Cl8	σ*	0.03112	4.67	0.88	0.057
C4-C5	σ		C5-C6	σ*	0.03	4	1.28	0.064
C4-H9	σ	1.97603	C2-C3	σ*	0.05369	3.75	1.05	0.057
C5-C6	π		N1-C2	π*	0.42741	17.09	0.26	0.061
C5-C6	π		C3-C4	σ*	0.02672	26.23	0.28	0.076
C5-C6	π		C10-F13	σ*	0.10152	7	0.5	0.023
C5-C10	σ		C4-C5	σ*	0.02232	1.6	1.25	0.04
C6-H11	σ	1.98065	N1-C2	σ*	0.03027	4.48	1.07	0.062
C10-F12	σ	1.99508	C5-C6	π*	0.32997	1.23	1.57	0.039
C10-F13	π	1.99379	C5-C6	π*	0.32997	0.99	1.02	0.031
C10-F13	σ	1.99379	C4-C5	σ*	0.02232	1.37	1.57	0.042
N1	σ	1.88933	C2-C3	σ*	0.05369	10.2	0.86	0.085
N1	σ	1.88933	C5-C6	σ*	0.03	8.69	0.9	0.08
Cl7	π	1.96483	N1-C2	π*	0.42741	1	1.46	0.034
Cl7	π	1.96483	N1-C2	π*	0.42741	5.99	0.84	0.063
Cl7	LP(2)	1.96483	N1-C2	σ*	0.03027	17.07	0.29	0.069
Cl8	LP(3)	1.91422	C3-C4	π*	0.33895	13.68	0.31	0.063
F12	LP(3)	1.93834	C5-C10	π*		5.8	0.78	0.06
F12	LP(2)	1.95444	C10-F13	σ*	0.10152	9.51	0.065	0.071
F12	LP(2)	1.95444	C10-F13	σ*	0.10152	10.92	0.66	0.076
F13	LP(2)	1.95279	C5-C10	σ*	0.05608	5.58	0.78	0.059
F13	LP(2)	1.95279	C10-F12	σ*	0.09247	10.21	0.65	0.073
F14	LP(3)	1.93774	C5-C10	σ*	0.05608	5.92	0.79	0.061
F14	LP(3)	1.93774	C10-F12	σ*	0.10152	11.23	0.63	0.077
F14	LP(3)	1.93774	C10-F13	σ*	0.10152	9.49	0.65	0.071

[a]$E^{(2)}$ means energy of hyper conjugative interaction (stabilization energy)
[b]Energy difference between donor and acceptor i and j NBO orbitals.
[c]F(i,j) is the Fock matrix element between i and j NBO orbitals

The Natural bond orbital analysis(NBO) unlock the secrets about stability, bonding, intramolecular charge transfer (ICT) and donor-acceptor relationship which are all collectively contribute to determine the electronic structure property of the title compound 2C5TFMP.The molecular stabilization can be explained by second order theory analysis [42]. The stabilisation of orbital interaction is proportional to the interaction is proportional to the energy difference between interacting orbitals. Therefore, the interaction having strongest stabilisation takes place between effective donors and effective acceptors. This bonding-antibonding interaction can be quantitatively described in terms of the NBO approach that is expressed by means of second order perturbation interaction energy $E^{(2)}$.This stabilisation energy $E^{(2)}$ associated with i donor →j(acceptor) delocalisation is estimated from the second order perturbation approach [43] as given in equation (5)

$$E^{(2)} = qi \frac{F^2(i,j)}{\epsilon_j - \epsilon_i} \qquad (5)$$

Where qi is the donor orbital occupancy, ϵ_i and ϵ_j are diagonal elements (orbital energies) and F (i,j) is the off-diagonal Fock matrix element.

Though several types of electronic interactions available between bonding, non-bonding and anti-bonding orbitals, the prominent stabilization includes lone pair л→σ* transition in 2C5TFMP.The highest stabilization about 26.23 kJmol^{-1} is observed at the interaction between (C5-C6) л→σ* (C3-C4).

The л→л* type of transition was observed at the interaction between C5-C6 and N1-C2 is about 17.09 kJmol^{-1}.

3.8 Hyperpolarizability and NLO activity

Nonlinear optics is to understand the nonlinear behaviour in the induced polarization and to analyze and to control its impact on the propagation of light in the matter [44].

In this work, the electronic dipole moment, molecular polarizability, anisotropy of polarizability and molecular first hyperpolarizability of the title compound were examined. The polarizability and hyperpolarizability tensors (αxx,αzy, αyy, αxz, αyz, αzz and βxxx, βxxy, βxyy, βyyy, βxxz, βxyz, βyyz, βxzz, βyzz and βzzz) can be obtained by a frequency job output file of Gaussian output are in atomic units (a.u.) (For α : 1a.u.= 0.1482× 10^{-24} esu; For β : 1a.u.=8.3×10^{-33} esu).The mean polarizability (α_{tot}), anisotropy of polarizability (Δα) and the average value of the first order hyperpolarizabilities (β_{tot})can be calculated using the equations (6),(7) and (8) [45].

$$\alpha_{tot} = \alpha xx + \alpha_{yy} + \alpha_{zz} / 3 \quad (6)$$

$$\frac{1}{\sqrt{2}} [(\alpha_{xx} - \alpha_{yy})^2 + (\alpha_{yy} - \alpha_{zz})^2 + (\alpha_{zz} - \alpha_{xx})^2 + 6\alpha^2_{xx}]^{1/2} \quad (7)$$

$$\beta = [(\beta_{xxx} + \beta_{xxy} + \beta_{xyy})^2 + (\beta_{yyy} + \beta_{xxz} + \beta_{yyz})^2 + (\beta_{xzz} + \beta_{yzz} + \beta_{zzz})^2]^{½} \quad (8)$$

In Table the figured parameters portrayed below and electronic dipole moment μ_i (i=x,y,z) and the total dipole moment μ for the title compound are recorded. The total dipole moment can be calculated utilizing the below equation (9).

$$\mu = \sqrt{\mu^2_x + \mu^2_y + \mu^2_z} \quad (9)$$

Table 7: The Calculated Electric dipole moment, Polarizability and First Hyperpolarizability of 2C5TFMP

Dipole Moment μ		Polarizability α			First order Hyperpolarizability β		
Parameter	**Value**	**Parameter**	**a.u**	**Esu (× 10^{-24})**	**parameter**	**a.u**	**Esu (×10^{-33})**
μ_x	0.2247	α_{xx}	-78.1724	-11.5851	β_{xxx}	-28.9363	249.981
μ_y	1.9603	α_{xy}	4.3592	0.646033	β_{xxy}	6.6916	57.8087
μ_z	-0.0653	α_{yy}	-64.6754	-9.58489	β_{xyy}	-16.0096	-1.38307
μ_{tot}	1.9742	α_{xz}	0.1159	171.764	β_{yyy}	9.5566	82.5595
		α_{yz}	-0.0025	3705	β_{xxz}	-0.0444	-0.38357
		α_{zz}	-70.1866	10.4017	β_{yyz}	0.8587	7.41831
			-71.0114	-10.524	β_{xzz}	-11.4101	-98.5719
					β_{yzz}	-2.5099	-21.683
					β_{zzz}	-0.6321	-5.46071
					β_{xyz}	-0.0800	-0.69112
					β	58.00666	5.0114 (×10^{-31})
First order Hyperpolarizability β						0.50114×10^{-30} esu	

The components of polarizability and the first hyperpolarizability of the present sample were exhibited in Table.7. The total dipole moment and first order hyperpolarizability are 1.9742 Debye and 0.50114×10^{-30} esu respectively and are shown in Table.7.Total dipole moment of title molecule is approximately 1.344 times greater than that of urea and first order hyperpolarizability is slightly greater than that of urea. So the result implies that this compound may have nonlinearity of the molecule.

3.10 UV-Vis Spectral Analysis

The Time-Dependant density functional theory (TD-DFT) calculation has been performed for 2C5TFMP on the basis of fully optimized ground state structure to investigate the electronic absorption properties. This method is able to detect accurate absorption wavelengths at a relatively small computing time. The most intense UV bands observed in Fig.13. Due to absorption from HOMO to LUMO, the significant peaks observed theoretically at 261.78, 254.34 and 241.05 nm. The electronic absorption spectra of the title molecule were figured in Table.8.The λmax is a function of substitution, the more electrons pushed into the ring, the larger λmax [46].

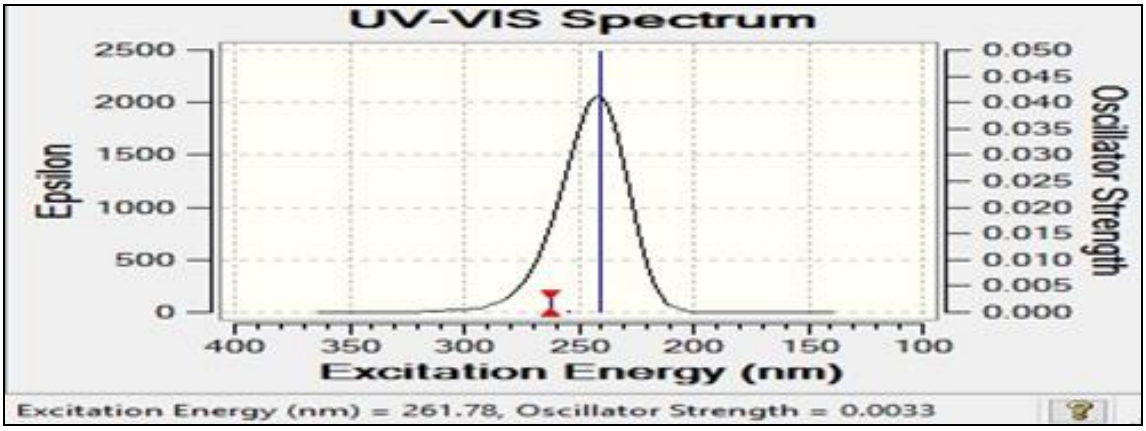

Fig 13: The UV-Visible Spectrum and excitation energy v/s oscillator strength of 2 C5TFMP

Table 8: Theoretical electronic absorption spectra values of 2C5TFMP

Excited State	Energy (eV)	Wavelength λ (nm)	Oscillator strengths (f)
1	4.7361	261.78	0.0033
2	4.8748	254.34	0.0002
3	5.1435	241.05	0.0497

3.11 NMR Spectroscopy

Nuclear magnetic resonance (NMR) is a research technique that is used in many disciplines of scientific research, medicine, various industries etc. The use of NMR and computer simulation methods offers a powerful way to interpret and predict the structure of large biomolecules [47]. For reliable calculations of magnetic properties, accurate prediction of molecular geometries are essential. Firstly, full geometry optimization of 2C5TFMP was performed at the Gradient corrected density functional level of theory using the hybrid B3LYP method [48].

For organic molecules, the ^{13}C NMR chemical shift appear in the range >100 ppm [49, 51]. In our present study, there are six carbon signals calculated theoretically and tabulated in Table.2, of which five carbons were located in aromatic region. The chemical shift value of carbon C2 is greater than other carbons due to the presence of the resonating effect of lone pair in the chlorine and the adjacent electronegative Nitrogen. The chemical shift value of C6 is the next higher due to the influence of electronegative nature of Nitrogen atom.

The proton chemical shift (^1H NMR) of organic molecules generally varies greatly with the electronic environment of the proton. Usually, Hydrogen attached to or nearby electron-withdrawing atom or group can decrease the shielding and move the resonance of attached proton towards a higher frequency, whereas electron-donating atom or group increases the shielding and moves the resonance towards a lower frequency [52].

In our present investigation, the molecule under study contains three hydrogen atoms. All the three atoms show the chemical shift in theoretical methods. The chemical shift of proton numbered H11 is highly towards the downfield when compare with other protons due to the influence of electronegative adjacent Nitrogen atom.

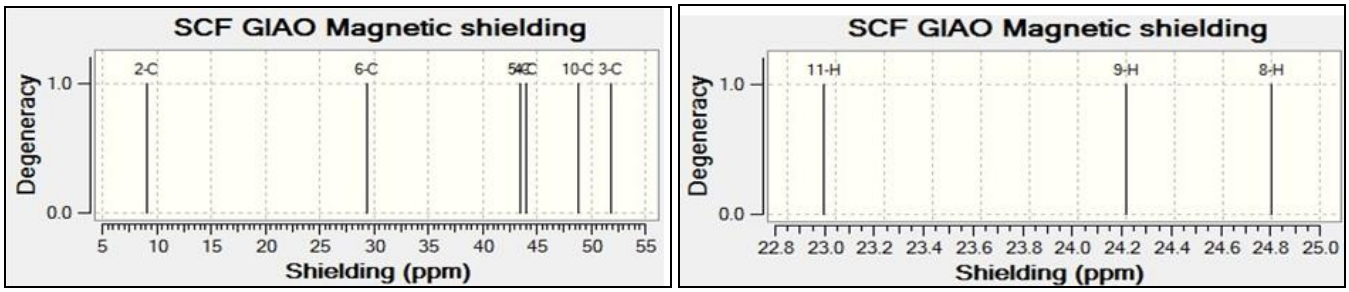

Fig 14: Theoretically calculated NMR spectrum of ^1H and ^{13}C for 2C5TFMP

Table 9: Theoretically calculated NMR spectra of ^1H & ^{13}C 2C5TFMP

Atom	Chemical Shift(ppm)
C2	173.288
C6	153.1082
C5	138.9866
C4	138.4167
C10	133.5756
C3	130.6109
H11	8.9324
H9	7.6839
H8	7.0804

4. Conclusion

Attempts have been made in the present work for the proper vibrational bands assignments for the compound 2C5TFMP from FTIR and FT Raman spectra. The equilibrium geometries and harmonic wavenumbers of 2C5TFM were determined and analyzed by B3LYP/6-311++G (d, p) basis set. The predicted harmonic frequencies were compared with the experimental data. NBO analysis has been shown that, the stabilization energies have been calculated from second order perturbation theory. The energies of one electron excitation from the highest occupied molecular orbital (HOMO) to the lowest unoccupied molecular orbital (LUMO) values are calculated from second order perturbation theory. The predicted harmonic frequencies were compared with the experimental data. Molecular electrostatic potential surfaces (MESP) together with the complete analysis of the vibrational spectra of IR, Raman and electronic spectra help to identify the chemically active sites of the molecule. The statistical thermodynamic parameters of 2C5TFMP for range of temperature 100 to 1000K were calculated theoretically computed wavenumbers in both the methods were found to be good agreement with experimental FT-IR and FT Raman results. Mulliken charge analysis and UV-Visible spectrum were also computed. The chemical shift shielding tensors are predicted by the computational NMR method. The dipole moment and hyperpolarizability result indicates that the title molecule may have NLO property.

5. References

1. Zeegers-Huyskens Th, Huyskens P, Ratajczak H, WJ Orville-Thomas Eds., Molecular Interactions, Wiley, Chichester, UK, 1981; 2:1.
2. Gur'yanova EN, Gol'dshtein IP, Perepelkova TI. Russ. Chem. Rev. 1976; 45:792-806.
3. Topacle A, Bayari Spectrochim S. Acta part A, 2001; 57:1385-1391.
4. Medhi RN, Berman R, Medhi KC, Jois SS. Spectrochim.

Acta Part A, 2000; 56:1523-1532.
5. Mohan S, Murugan R. Ind. J. Pure Appl. Phys., 1992; 30:283-286.
6. Krishnakumar V, John R. Xavier, Spectrochim. Acta A, 2005; 61:253-260.
7. Tripathi RS, Indian J. Pure and Appl. Phys., 1973; 11:277-279.
8. Sortur V, Yenagi J, Tonannavar J, Spectrochim. Acta A, 2008; 69:604-611.
9. Lizarraga ME, Navarro R, Urriolabeitia EP. J Org. met. Chem., 1997; 542:51-60.
10. Georgopoulou AS, Ulvenlund S, DMP Mingos. I Baxter and DJ Williams, J. Chem. Soc., 1999; 4:547-551.
11. Liaw W, Lee, Chen C, Lee C, Lee G, Peng S. J Am. Chem Soc., 2000; 122:488-494.
12. Frisch MJ *et al.*, Gaussian 09, Revision A. 9, Gaussian, Inc., Pittsburgh, 2009.
13. Schlegel HB. J Comput. Chem., 1982; 3:214-218.
14. Kalsi PS. Spectroscopy of Organic Compounds, Sixth ed., New Age International p Limited Publishers, New Delhi, 2005.
15. Socrates G. Infrared and Raman Characteristic group frequencies, Tables and Charts, third ed., Wiley, Chichester, 2001.
16. Rauhut G, Pulay P. J Phys. Chem., 1995; 99:3093-3100.
17. Fogarasi G, Pulay P. In JR Durig Ed., Vibrational Spectra and Structure, Elsevier, Amsterdam, 1985; 14:125-219.
18. Sundius T, Vib. Spectrosc, 2002; 29:89-95.
19. Frisch A, Nielson AB, Holder AJ. Gaussview Users Manual, Gaussian Inc., Pittsburgh, PA, 2000.
20. Sharma YR. Elementary Organic Spectroscopy, Principles and Chemical Applications: S. Cgande abd Company Ltd., New Delhi, India, 1994, 92-93.
21. Kalsi PS. Spectroscopy of Organic Compoubds, 6thedn Wiley Eastern Limited, New Delhi, India, 2004.
22. Seshadri S, Sangeetha R, Rasheed MP, Padmavathy M. International Research Journal of Engineering and Technology IRJET, 2016, 03.
23. Singh RN, Prasad SC. Vibrational spectra of isomeric bromoxylenes. Spectrochemica Acta A, 1974, 34:39.
24. Prabhavathy N, Senthilnayaki N, Phys. Express., 2014; 4(12):1-15.
25. Socrates G. Infrared and Raman Characteristics Group Frequencies, Wiley, New York, USA, 2000.
26. Bellamy LJ. Advances in Infrared Group frequencies, Barnes and Noble Inc., USA, 1968.
27. Ramalingam S, Periandy S, Govindarajan M, Mohan S. Spectrochim. Acta Part A, 2010; 75:1552.
28. Gunasekaran S, Seshadri S, Muthu S, Ind J. Pure and Appl. Phys., 2006; 44:360.
29. Mooney EF, Spectrochemica Acta, 1964; 20:1021.
30. Balachandran V, Murali MK, Elixir Vib. Spec., 2011; 40:5105.
31. Irikura KK, THERMO PL. National Institute of Standards and Technology, Gaithersburg, MD, 2002.
32. Bevan J. Ott and J Boerio-Goates, Chemical Thermodynamics: Principles and Applications, Academic Press,
33. San Diego, 2000.
34. Singh P, Singh NP, Yadav RA. J Chem. Pharm. Res. 2010; 2(6):199.
35. Zhang R, Dub B, Sun G, Sun Y. Spectrochim. Acta A, 2010; 75:1115-1124.
36. Govindarajan M, Karaback M. Journal of Molecular Structure, 2013; 1038:114-125.
37. Choudhary N, Bee S, Gupta A, Tandon P. Comp Theor Chem., 2013; 1016:8-21.
38. Dixit, Yadav, Biochem Pharmacol Los Angel, 2015.
39. Becke D. J Chem. Phys, 1993; 98:5648e5652.
40. Socrates G. Infrared and Raman Characteristic Group Frequencies e Tables and Charts, third ed., John Wiley & Sons, Chichester, 2001.
41. Sangeetha R, Seshadri S, Rasheed MP. IJOAR, 2017; 05(5).
42. Arivazhagan M, Senthil J, Kumar. Indian Journal of Pure & Applied Physics, 2012; 50:363-373.
43. Weinhold F, Landis CR. Valency and Bonding: A Natural Bond Orbital Donor-Acceptor Perspective. Cambridge University Press, 2005.
44. Weinhold F, Landis CR. Natural Bond Orbitals and extensions of localized bonding concepts. Chem Educ Res Pract., 2001; 2:91-104.
45. Arivuoli D. Pramana Journal of physics, 2001; 57:871-883.
46. Seshadri S, Rasheed MP, Sangeetha R. IOSR Journal of Applied Physics, 2015; 7(6):56-70.
47. Raja M, Raj R, Muhamed S, Muthu M. Suresh, Journal of Molecular Structure, 2017; 1128:481-492.
48. Schlick T, Molecular Modeling, Simulation. An Interdisciplinary Guide, second ed., Springer, New York, 2010, 21.
49. Sangeetha R, Seshadri S, Rasheed MP. International Journal of Advanced Engineering and Research Development, 2017; 4(08).
50. Kalinowski HO, Berger S, Brawn S. Carbon-13NMR Spectroscopy, John Wiley and Sons, Chichester, 1988.
51. Pihlajer K, Kleinprter E. Eds., Carbon-13Chemical Shifts in Structure and Spectrochemical Analysis, VCH publishers, Deerfield Beach, 1994.
52. Varsanyi G. Vibrational Spectra of Benzene Derivatives, Academic press, New York, 1969.
53. Subramania N, Sundaraganesan N, Jayabharathi J. Molecular Structure, spectroscopic FT-IR, FT-Raman, NMR, UV studies and first-order molecular hyperpolarizabilities of 1,2-bis(3-methoxy-4-hydroxybenzyli dene) hydrazine by density functional method, Spectrochim. Acta A. 2010; 76(2):259-269.